Traveling Wave Transport of Particles and Particle Size Classification

Hiroyuki Kawamoto, Naoto Hasegawa and Kyogo Seki
Department of Mechanical Engineering, Waseda University
Shinjuku, Tokyo, Japan

Abstract

A basic research is being carried out on transport of particles and particle size classification in electrostatic traveling field. A particle conveyor consisting of parallel electrodes was constructed and four-phase traveling electrostatic wave was applied to the electrodes to transport particles on the conveyer. The following were clarified by the experiment and numerical simulation with the Distinct Element Method: (1) Particles were transported almost linearly with time. A transport rate was also linear with the applied voltage but a threshold existed due to adhesion force. (2) The direction of particle transport did not always coincide with that of the traveling wave but partially changed depending on the frequency of the traveling wave, the particle diameter, and the electric field. Particles were vibrated but not transported under high frequency field. (3) Particles were efficiently transported under conditions of low frequency, high voltage, and the application of rectangular wave. (4) Particles were classified with size under the voltage application of appropriate frequency.

Introduction

The idea to transport particles with electrostatic traveling waves was first conceived by Masuda.[1] Utilization of a traveling wave conveyor for the particle transport has the advantage that the transport can be controlled through electrical parameters instead of mechanical means.[2-4] We are conducting a basic research on this technology to utilize it for the transport of toner and carrier particles in laser printers.[5,6] In this investigation, because we discovered particles were classified with size utilizing this technique, it is also presented in this report.

Experimental

A conveyor and a power supply used for experiments are shown in Fig. 1. The conveyor consists of 125 parallel copper electrodes, 1 mm width and 2 mm pitch, etched by photolithography on a plastic substrate, 120 mm width and 250 mm length, as shown in Fig. 2. The surface of the conveyor is covered with an insulating film made of acetate rayon (3M, 810-18D) to prevent from electrical breakdown between electrodes.

Traveling wave propagation is achieved utilizing four amplifiers (Matsusada Precision Inc, Tokyo, HOPS-1B3) and five function generators (IWATSU, Tokyo, SG-4105), one of which is used to control phase-differences of the other four generators. Not only rectangular, as added in Fig. 1, but also sine and triangular waves are generated by the function generators.

Four kinds of spherical carrier particles made by the polymerization method (Toda Kogyo) were used for experiments. Specifications of particles are listed in Table 1 and photographs are shown in Fig. 3.

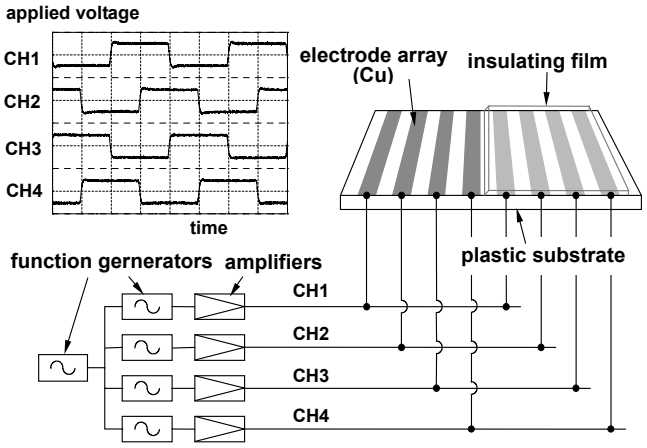

Figure 1. Particle conveyer and power supply.

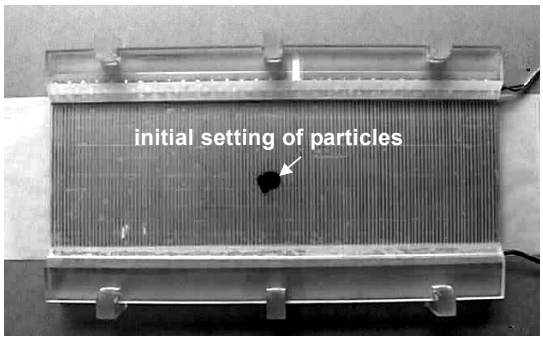

Figure 2. Photograph of particle conveyer.

Table 1. Specification of particles.

	ACM 235	ACM 255	ACM 288	ACM 2107
averaged diameter, μm	29.7	47.4	72.6	106.3
standard deviation, μm	5.3	11.8	23.3	13.1
density, kg/m^3	3.50	3.52	3.62	3.50
resistivity, Ωcm	1×10^9	2×10^7	3×10^9	8×10^7

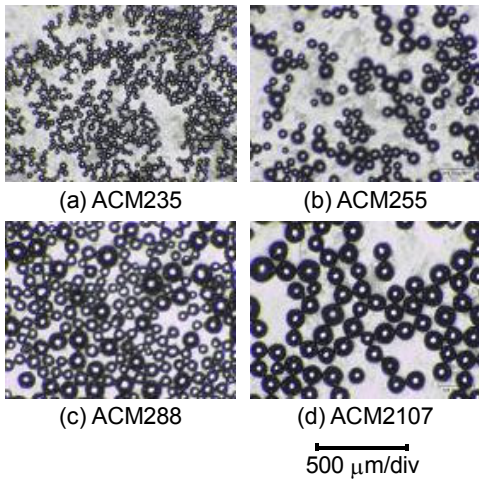

Figure 3. Photograph of particles used for experiment.

Fundamental Characteristics

Transport Rate

In the first place, transport rate was measured with the following steps. First, cloud of 0.5-gram particle was mounted at the position of 40 mm from the left end of the conveyor and rectangular wave of 1.0 Hz was applied to electrodes. Then the weight of particles overflowed from the right end of the conveyer was measured by an electric balance at every five seconds. Some examples of experimental results are shown in Fig. 4. The transport rate is the accumulated weight overflowed from the edge of the conveyer to the initially settled weight. Because some particles adhered to the insulating film on the conveyer and not transported, the final transport rate was less than unity. It is recognized that the transport rate is almost linear with time.

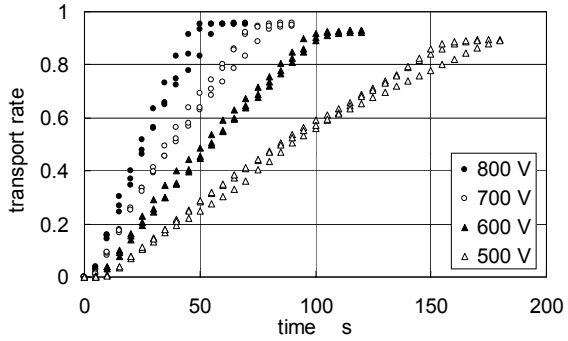

Figure 4. Transport rate of particles with time. (ACM 2107, 1 Hz, rectangular wave)

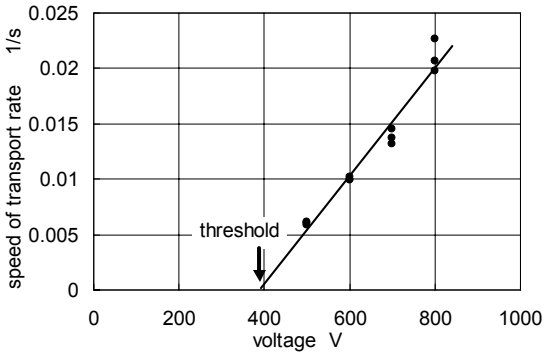

Figure 5. Applied voltage vs. speed of transport rate. (ACM2107, 1 Hz, rectangular wave)

Figure 5 shows applied voltage versus a speed of the transport rate, time differential of the transport rate. The speed of the transport rate was linearly increased to the applied voltage but a threshold voltage existed. The threshold might be determined by the adhesion and static friction force between particles and the insulation film.

Transport Direction

At low frequency operation, particles were transported to the common direction with that of the traveling wave and the motion was synchronized with the wave speed. However, at high frequency some particles delayed to the wave and moved to the opposite direction. To examine characteristics associated with the direction of the particle transport, we implemented the following experiments. First, cloud of 0.5-gram particles was mounted at the center of the conveyor and ±800 V rectangular wave was applied to electrodes. Then we measured the weight of particles transported forward, backward, and not transported in 30 seconds, where 'forward' is the same direction with that of the traveling wave and 'backward' is the opposite direction. The measured rate at each frequency is summarized in Fig. 6. There are three modes with respect to the transport direction.

(I) Forward Transport Mode: Particles were transported forward when the frequency was low, less than 100 Hz in the case of Fig. 6. A transport speed was almost synchronized with the wave speed and almost all particles were transported to the forward direction. Small particles were apt to be transported forward even at high frequency.

(II) Backward Transport Mode: Particles were transported backward at medium frequency, 150 – 250 Hz in the case of Fig. 6. The transport speed was one-forth of the wave speed. All particles were not transported backward but some particles stayed on the conveyer.

(III) Non-Transported Mode: Particles were not transported at high frequency, more than 400 Hz in the case of Fig. 6, but vibrated on the conveyer and only diffused at the initial setting point. Large particles were generally not transported and stayed on the conveyer even at relatively low frequency, however, the non-transport rate of very small particles, ACM235, was large, because relative adhesion force to the film was large for small particles.

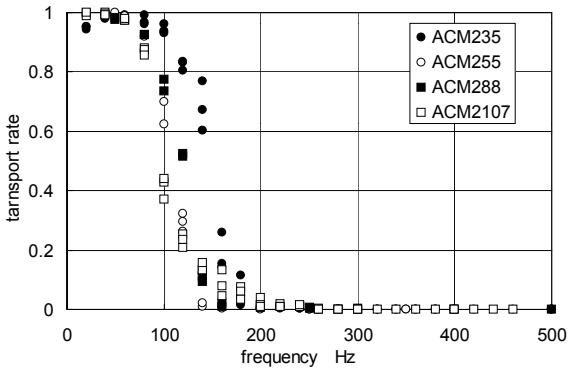

(a) forward

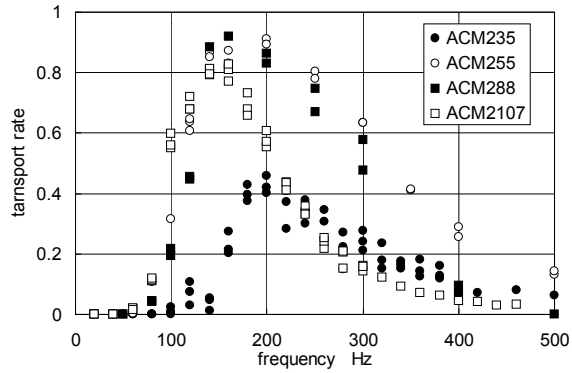

(b) backward

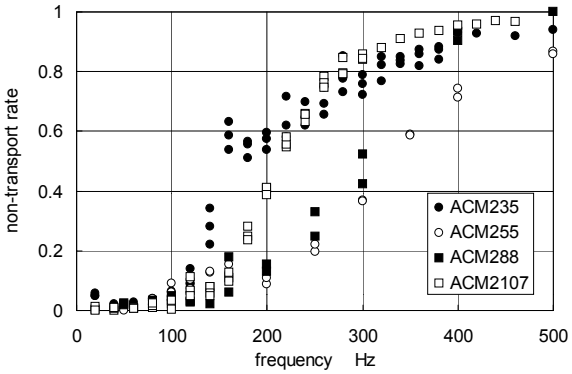

(c) non-transported

Figure 6. Rate of forward, backward, and non-transported particles with respect to frequency of traveling wave. (800 V, rectangular wave)

Figure 7 illustrates rates of three modes of one kind of particles. Summation of the three rates is unity. It is clearly recognized that particles were transported forward at low frequency, but some particles moved backward and some were not transported at medium frequency, and almost all particles were not transported at high frequency.

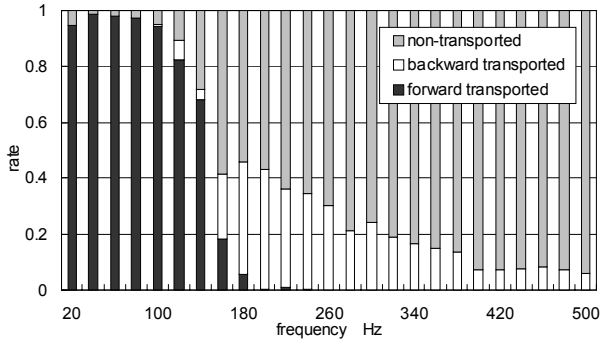

Figure 7. Rates of forward, backward, and non- transported particles with respect to frequency of traveling wave. (ACM235, 800 V, rectangular wave)

Similar experiments were conducted with the parameter of the applied voltage. The result is shown in Fig. 8. Because the Coulomb force to particles were large in the high electrostatic field, particle motion was synchronized with the electrostatic wave and transported forward even at high frequency. Therefore, high voltage operation is preferable for the efficient transportation, although it is restricted by the insulation breakdown between electrodes. Threshold voltage of our conveyer was 800 V.

Figure 9 shows the effect of waveforms; rectangular, sine, and triangular. Experiments were conducted with the common peek voltage, not rms., because maximum voltage is determined by its peek value due to the electrical breakdown. It is obvious that the rectangular wave is most effective.

Numerical Simulation

Numerical calculation was conducted to simulate the transport process. Two-dimensional Distinct Element Method (DEM) was used for the calculation of particle dynamics in the electrostatic field.[7] In the calculation the motion and momentum equations were solved with three degrees of freedom, (x,y,θ) for each bead i, where $\boldsymbol{x} = (x,y)$ are displacements in the Cartesian coordinates and θ is a rotational angle.

$$m_i\ddot{\boldsymbol{x}}_i = \boldsymbol{F}_{ei} + \boldsymbol{F}_{dipole\,i} + \boldsymbol{F}_{mechanical} + \boldsymbol{F}_{airdrugi} + m_i\boldsymbol{g}\,, \qquad (1)$$

$$I_i\ddot{\theta}_i = M_{friction_i} + M_{mechanical_i}\,, \qquad (2)$$

where m is a mass and I is an inertia of particle. The following forces and moments were included in the equations; electrostatic force to charged particles $\boldsymbol{F}_e$, electrostatic force to polarized particles assumed to be dipoles in the gradient electrostatic field $\boldsymbol{F}_{dipole}$,[8] force due to air drug $\boldsymbol{F}_{airdrug}$, gravitational force m$\boldsymbol{g}$, force and moment due to mechanical contact between bead and floor $\boldsymbol{F}_{mechanical}$, $M_{mechanical}$ (refer to Fig. 10), and momentum drag due to rolling friction $M_{friction}$. Mechanical and electrostatic interactions between particles were neglected.

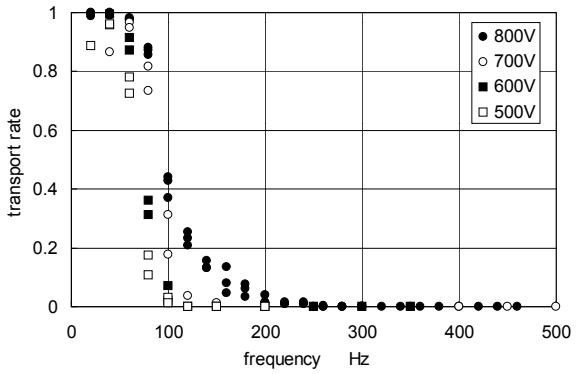

(a) forward

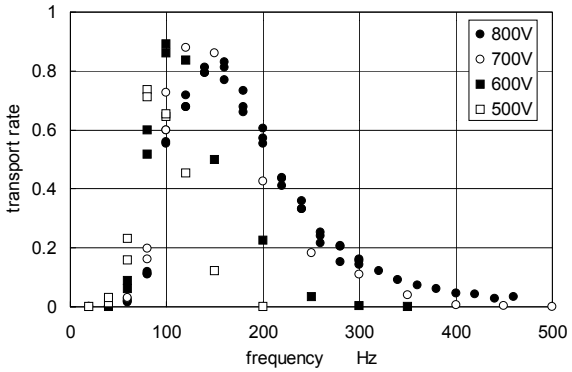

(b) backward

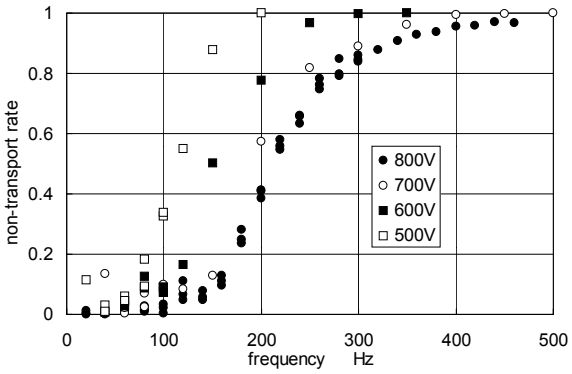

(c) non-transported

Figure 8. Rate of forward, backward, and non-transported particles with respect to frequency of traveling wave. (ACM2107, rectangular wave)

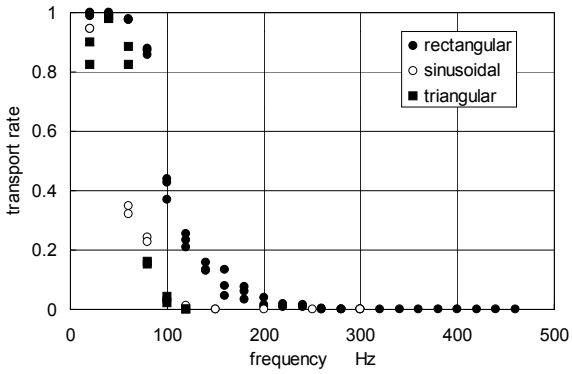

(a) forward

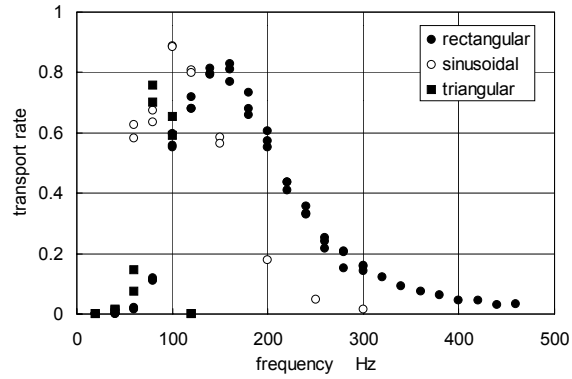

(b) backward

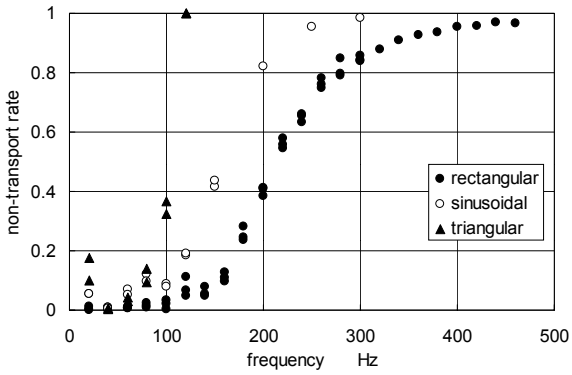

(c) non-transported

Figure 9. Rate of forward, backward, and non-transported particles with respect to frequency of traveling wave. (ACM2107, 800 V)

$$\boldsymbol{F}_e = q\boldsymbol{E}, \quad \boldsymbol{F}_{dipole} = 4\pi\varepsilon_0 \frac{\varepsilon - 1}{\varepsilon + 2} R^3 \boldsymbol{E}\nabla E \tag{3}$$

$$\boldsymbol{F}_{airdrug} = 6\pi\eta R\dot{\boldsymbol{x}}, \quad M_{friction} = 1.5F_n^{1.5}\dot{x}$$

where q is charge of particle, $\boldsymbol{E}$ is the electrostatic field, ε_0 is the permittivity of free space, ε is a relative permittivity, R is the radius of particle, η is a viscosity, and F_n is a normal force to particle in contact with the floor.

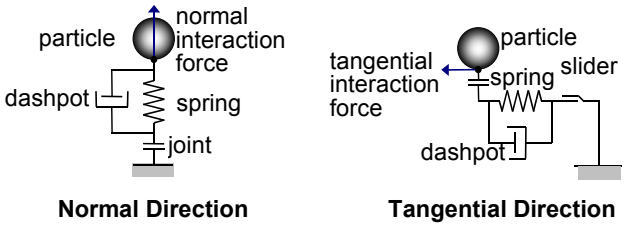

Figure 10. Mechanical interaction based on Distinct Element Method. The mechanical interaction force is calculated by the Hertz's formula.

Electrostatic field was calculated using two-dimensional Finite Element Method, where a periodical boundary condition was employed at every two parallel electrodes and the domain was meshed in square elements of secondary degree, because the gradient of electrostatic field, which is necessary to calculate Eq. (4), is constant in the quadric element.

$$\nabla^2\phi = 0, \quad \boldsymbol{E} = -\nabla\phi \tag{4}$$

Calculated distributions of the potential ϕ and the electrostatic field $\boldsymbol{E}$ are shown in Fig. 11.

Figure 12 illustrates the numerical result on the transport direction corresponds to the preceding experiment shown in Fig. 6, i.e., dynamics of forty 47 μm diameter particles were simulated under the condition of rectangular ±800 V wave. Non-transported particles were not included into the result. Charge of each particle is assumed to be 0.092 μC/g. It is clearly recognized that particles are transported in forward direction at low frequency but they move to backward at the frequency more than a critical. This characteristic qualitatively agreed with the experimental observation. However, calculated critical frequency, 60 Hz, did not agree with the measured, 100 Hz. Because the critical frequency depends highly on the charge of particles, as shown in Fig. 13, we are planning to measure charge of particles after transport operation. Numerical model must also be brushed up, for example, both mechanical and electrostatic interactions between particles must be included in the model and the field must be three-dimensional.

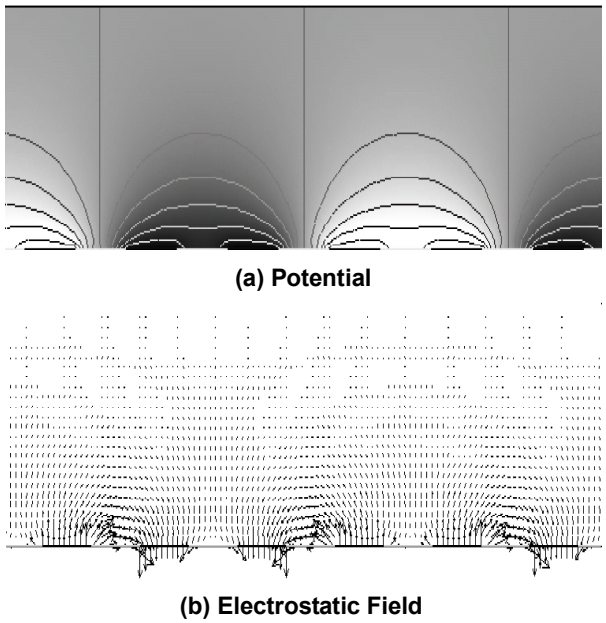

Figure 11. Calculated distributions of potential and electrostatic field.

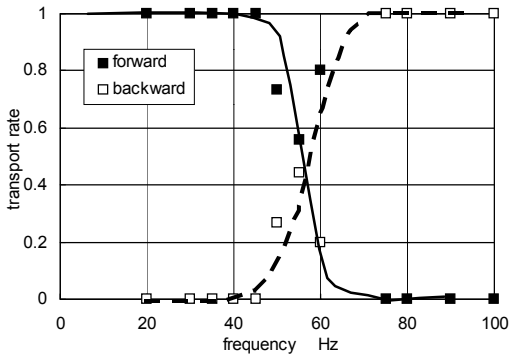

Figure 12. Calculated rate of forward and backward particles with respect to frequency of traveling wave. (forty particles of 47-μm diameter, 800 V, rectangular wave)

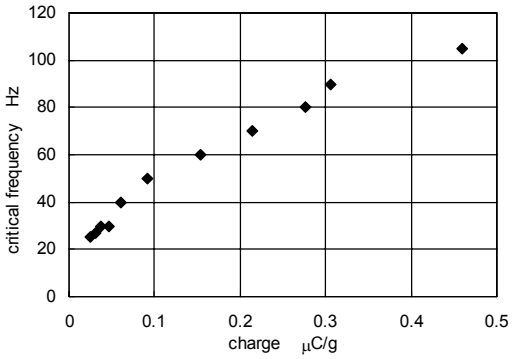

Figure 13. Calculated critical frequency with respect to charge of particles (forty particles of 47 μm diameter, 800 V, rectangular wave)

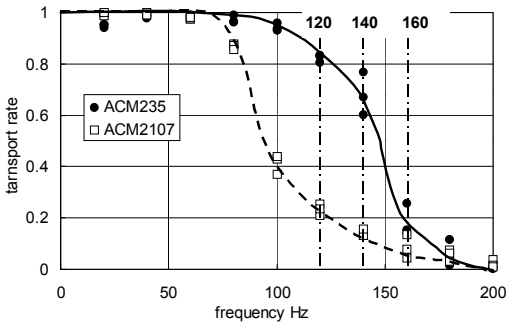

Figure 14. Rate of forward transported particles with respect to frequency of traveling wave. (800 V, rectangular wave)

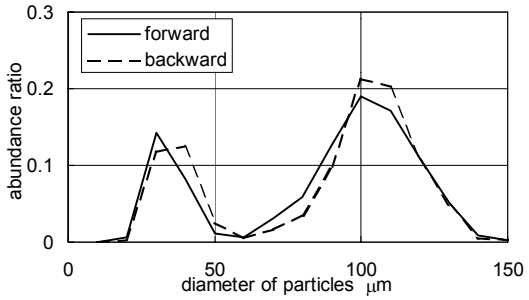

(a) 120 Hz

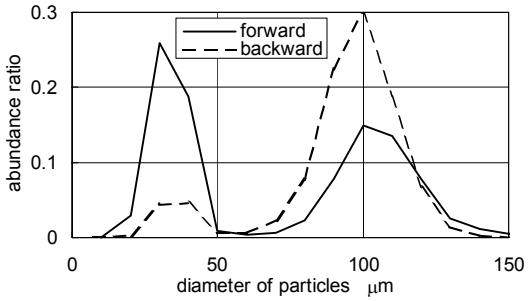

(b) 140 Hz

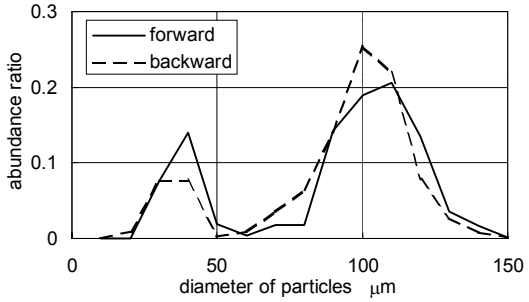

(c) 160 Hz

Figure 15. Distributions of particle diameter in forward and backward transported particles. (ACM235+ ACM2107 mixed particles, 800 V, rectangular wave)

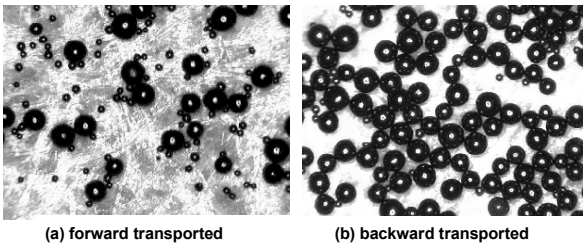

Figure 16. Photographs of forward and backward trans-ported particles. (ACM235+ACM2107 mixed particles, 800 V, 140 Hz, rectangular wave)

Particle Classification

An interest finding of the experiment was that a transition frequency from the forward to the backward transported region depended on the particle size, i.e., although small particles were transported to the forward direction even at relatively high frequency operation, large particles delayed and moved to backward at lower frequency. This feature suggested that particles could be classified with size with the application of traveling wave of an appropriate frequency. Figure 14 shows the measured forward transported rates of the small particle ACM235 and the large particle ACM2107. The results indicated that the rate of forward transport depended not only on the wave frequency but also on the particle diameter, that is, at an appropriate frequency smaller particles were transported forward, otherwise larger particles were transported backward. To demonstrate the hypothesis we prepared mixed particles of particle ACM235 and ACM2107, the number of each one being the same. Under the condition of the optimum frequency, 140 Hz in this case, a significant classification was realized as shown in Fig. 15. We can also confirm the classification by the photograph shown in Fig. 16.

Figure 17 shows another evidence on the particle classification with particle ACM288 whose diameter was distributed in wide range (refer to Table 1). The classification was also realized as shown in Figs. 17 and 18.

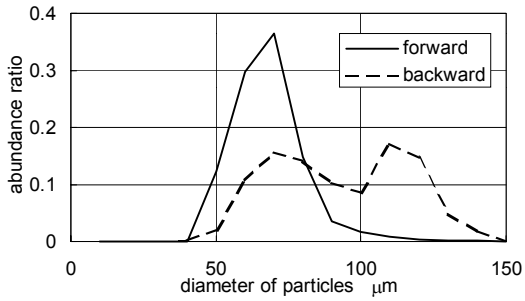

Figure 17. Distributions of particle diameter in forward and backward transported particles. (ACM288, 800 V, 140 Hz, rectangular wave)

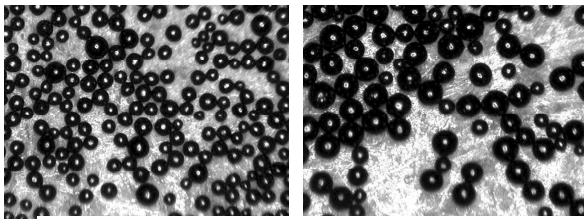

Figure 18. Photographs of forward and backward trans-ported particles. (ACM 288, 800 V, 140 Hz, rectangular waver)

Concluding Remarks

A basic research was carried out on transport of particles and particle size classification in electrostatic traveling field. The following were deduced from the investigation.

(1) Particles were transported almost linearly with time. A transport rate was also linear with applied voltage but a threshold existed due to adhesion force. The most effective transport was achieved under the application of high rectangular voltage at low frequency.

(2) The transport directions were categorized with three features, forward, backward, and non-transported. At low frequency, particles were transported in the direction of the traveling wave propagation (forward direction), otherwise at relatively high frequency particles transported backward increased. Motion of forward transported particles was synchronized with the traveling wave but that of backward was 1/(phase numbers) of the wave. Particles were not transported but only vibrated at higher frequency, herein a limitation for the transport existed.

(3) Utilizing the difference of the critical frequency with respect to the particle size, we demonstrated particle classification with size.

(4) The two-dimensional DEM simulation was qualitatively in good agreement with the experiments on the characteristic associated with frequency of traveling wave. However, it is essential to estimate the amount of charge precisely by experiment, because it largely influences on particle dynamics.

Acknowledgment

This work is supported by The Ogasawara Foundation for the Promotion of Science & Engineering.

References

1. S. Masuda, K. Fujibayashi, K. Ishida, H. Inaba, Confinement and transportation of charged aerosol clouds via electric curtain, *Trans. of the Institute of Elcc. Eng. Japan*, Vol. 92-B, No.1 (1972) pp.9-18.
2. F. M. Moesner and T. Higuchi, Electrostatic Devices for Particle Microhandling, *IEEE Trans. Industry Applications*, Vol. 35, No. 3 (1999) pp.530-536.
3. R. Kober, Traveling Wave Transport of Conductive Toner Particles, *IS&T's NIP16: Int. Conf, on Digital Printing Technologies* (2000) pp.536-539.
4. K. Taniguchi, Improved Driving Characteristics for the Toner Transportation System, *IS&T's NIP16: Int. Conf. on Digital Printing Technologies* (2000) pp.540-542.
5. E. M. Williams, The Physics and Technology of Xerographic Processes, Krieger Publishing, FL (1993).
6. L. B. Schein, Electrophotography and Development Physics (Revised Second Edition), Laplacian Press, CA (1996).
7. N. Nakayama, H. Kawamoto and M. Yamaguchi, Statics of Magnetic Bead Chain in Magnetic Field, *J. Imaging Sci. Technol*, Vol. 46, No. 5 (2002) pp.422-428.
8. T. Jones, Electromechanics of Particles, Cambridge University Press (1995).

Biography

Hiroyuki Kawamoto holds a BS degree in Electrical Engineering from Hiroshima Univ. (1972) and a Dr. degree in Mechanical Engineering from Tokyo Institute of Technology (1983). From 1972 to 1991 he was a Senior Engineer at the Nuclear Division of Hitachi Ltd. In 1991 he moved to Fuji Xerox, and had been engaged in the research of electrophotography as a Research Fellow. In 1999 he left Fuji Xerox and he is now a professor of Waseda Univ. His awards include the Japan Society of Mechanical Engineers Young Scientist Award (1984), the 7th International Microelectronics Conf. Best Paper Award (1992), the Japan Institute of Invention and Innovation Patent Award (1993), and the 10th International Symposium on Applied Electromagnetics and Mechanics Award for Outstanding Presentation Paper (2001). He was selected a Fellow of the IS&T in 1999.